Accepted Manuscript

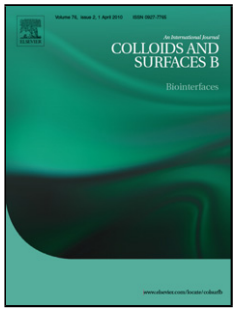

Title: Surface engineering of silica nanoparticles for oral insulin delivery: characterization and cell toxicity studies

Author: Tatiana Andreani Charlene P. Kiill Ana Luiza R. de Souza Joana F. Fangueiro Lisete Fernandes Slavomira Doktorovová Dario L. Santos Maria L. Garcia Maria Palmira D. Gremião Eliana B. Souto Amélia M. Silva

PII: S0927-7765(14)00597-9
DOI: http://dx.doi.org/doi:10.1016/j.colsurfb.2014.10.047
Reference: COLSUB 6711

To appear in: *Colloids and Surfaces B: Biointerfaces*

Received date: 22-9-2014
Revised date: 19-10-2014
Accepted date: 22-10-2014

Please cite this article as: T. Andreani, C.P. Kiill, A.L.R. Souza, J.F. Fangueiro, L. Fernandes, S. Doktorovová, D.L. Santos, M.L. Garcia, M.P.D. Gremião, E.B. Souto, A.M. Silva, Surface engineering of silica nanoparticles for oral insulin delivery: characterization and cell toxicity studies, *Colloids and Surfaces B: Biointerfaces* (2014), http://dx.doi.org/10.1016/j.colsurfb.2014.10.047

Surface engineering of silica nanoparticles for oral insulin delivery: characterization and cell toxicity studies

Tatiana Andreani[a,b,c], Charlene P. Kiill[d], Ana Luiza R. de Souza[d], Joana F. Fangueiro[c,e], Lisete Fernandes[f], Slavomira Doktorovová[g], Dario L. Santos[a,b], Maria L. Garcia[h], Maria Palmira D. Gremião[d], Eliana B. Souto[i], Amélia M. Silva[a,b*]

[a]Department of Biology and Environment, University of Trás-os Montes e Alto Douro,UTAD, Quinta de Prados, 5001-801, Vila Real, Portugal

[b]Centre for Research and Technology of Agro-Environmental and Biological Sciences, CITAB, UTAD, Vila Real, Portugal

[c]Fernando Pessoa University, UFP, Praça 9 de Abril, 349, 4249-004, Porto, Portugal

[d]Faculty of Pharmaceutical Sciences, Universidade Estadual Paulista, UNESP, Rodovia Araraquara-Jau, Km. 01, Araraquara, São Paulo, Brazil

[e]Research Centre for Biomedicine, CEBIMED, Fernando Pessoa University, UFP, Porto, Portugal

[f]Electron Microscopy Unit, UTAD, Vila Real, Portugal

[g]Research Institute For Medicines and Pharmaceutical Sciences – iMed.UL, Faculty of Pharmacy, University of Lisbon, Av. Prof. Gama Pinto, 1649-003, Lisbon, Portugal

[h]Department of Physical Chemistry, Faculty of Pharmacy, Barcelona University, Av. Joan XXIII s/n, 08028 Barcelona, Spain

[i]Departament of Pharmaceutical Technology, Faculty of Pharmacy, University of Coimbra (FFUC), Pólo das Ciências da Saúde, Azinhaga de Santa Comba, 3000-548 Coimbra, Portugal

* Corresponding author:
Amélia M. Silva
Department of Biology and Environment, School of Life and Environmental Sciences, University of Trás-os-Montes and Alto Douro, Quinta de Prados; 5001-801 Vila Real; Portugal
E-mail: amsilva@utad.pt
Phone: +351 259350106; Fax: +351-259350480

Abstract

The present work aimed at studying the interaction between insulin and SiNP surfaced with mucoadhesive polymers (chitosan, sodium alginate or polyethylene glycol) and the evaluation of their biocompatibility with HepG2 and Caco-2 cell lines, which mimic *in vivo* the target of insulin-loaded nanoparticles upon oral administration. Thus, a systematic physicochemical study of the surface-modified insulin-silica nanoparticles (Ins-SiNP) using mucoadhesive polymers has been described. The surfacing of nanoparticle involved the coating of silica nanoparticles (SiNP) with different mucoadhesive polymers, to achieve high contact between the systems and the gut mucosa to enhance the oral insulin bioavailability. SiNP were prepared by a modified Stöber method at room temperature via hydrolysis and condensation of tetraethyl orthosilicate (TEOS). Interaction between insulin and nanoparticles was assessed by differential scanning calorimetry (DSC), X-ray and Fourier-transform infrared (FTIR) studies. The high efficiency of nanoparticles' coating resulted in more stable system. FTIR spectra of insulin-loaded nanoparticles showed amide absorption bands which are characteristic of α-helix content. In general, all developed nanoparticles demonstrated high biocompatible, at the tested concentrations (50 – 500 μg/mL), revealing no or low toxicity in the two human cancer cell lines (HepG2 and Caco-2). In conclusion, the developed insulin-loaded SiNP surfaced with mucoadhesive polymers demonstrated its added value for oral administration of proteins.

Keywords: silica nanoparticles,coated-SiNPs, insulin,mucoadhesive polymersHepG2 cell, Caco-2 cell

1. Introduction

The recent advances in the field of biotechnology has shown several innovative strategies for protein drug delivery, exploiting non-invasive routes (e.g. oral [1, 2], nasal [3], pulmonary [4, 5], buccal [6, 7] or transdermal [8]), to reach a better patient's compliance in the treatment of diabetes. Among the proposed non-invasive alternatives, the oral administration of insulin seems to be more convenient to the patient. Insulin could be rapidly delivered in the liver through the portal circulation, after being absorbed in the intestine and, thus, the hyperinsulinemia condition could be avoided [9]. Nevertheless, the oral absorption of therapeutic proteins is hindered by several difficulties, such as their high molecular weight and hydrophilicity, low pH of gastric medium leading to protein denaturation and the presence of proteolytic enzymes that can reduce or even abolish their performance *in vivo* [10].

A promising strategy to improve the oral insulin bioavailability is to develop drug delivery systems that protect the protein from metabolic degradation, as well as prolong the gastrointestinal residence time, improving the absorption of the macromolecules through the intestinal tract. Nanoparticles coated with selected mucoadhesive polymers would be advantageous for oral delivery of therapeutic proteins.

Due to their high porosity, specific surface area, biocompatibility and ease of surface functionalization, silica nanoparticles (SiNP) have been considered an excellent option as delivery systems for proteins [11-14].The presence of residual silanol groups (Si-OH) onto the silica surface triggers the reactive sites for its surface modification by specific organic groups [15].

Based on these previous considerations, the purpose of the present study was to develop and characterize an organic/inorganic hybrid system intended for the oral insulin administration by combining the advantages of SiNP with the mucoadhesive properties of selected hydrophilic polymers. In this work, SiNP were chosen as drug delivery system for insulin, using chitosan (CH), sodium alginate (SA) or poly(ethylene glycol) (PEG) as mucoadhesive polymers. Multifunctional polymers have been extensively explored as matrix material in the development of mucosal drug delivery systems [16]. Chitosan is a biocompatible polysaccharide which improves the penetration of therapeutic proteins in the intestinal mucosa, because of the interaction of its amine

groups with negatively charged mucin. Chitosan can increase the paracellular permeability by affecting the structure of proteins associated to the tight junctions [17]. Alginate is a biopolymer also showing bioadhesive properties. Unlike chitosan, alginate prolongs the drug residence time in the mucosa due to the presence of numerous carboxyl groups, leading to a strong bioadhesive interaction by hydrogen bonds between anionic polymer and mucin [18].

PEG-coated nanoparticles have also been investigated for oral administration. It is known that PEG coatings can stabilize the nanoparticles in the gastric and intestinal fluids by steric hindrance, due to the inhibition of plasma protein adsorption [19]. In addition, PEGs can promote the mucoadhesion by the penetration of their chains in the intestinal mucosa [20].

Despite the increased attractiveness of nanotechnology for biomedical applications, the human exposure and environmental impact of the nanomaterials are also of great concern. Recent studies show that intrinsic properties of nanoparticles, such as size, shape and surface charge, can damage the cell membrane leading to changes of cell morphology and stability [21]. Therefore, it is important to consider a balance between the benefits and the potential hazards of nanomaterials when developing a suitable system for the purpose of drug and targeting delivery.

In the present study, the interaction between insulin and SiNP coated with different mucoadhesive polymers was examined by X-ray diffraction, differential scanning calorimetry (DSC) and Fourier transform infrared (FTIR) analyses. The biocompatibility of different nanoparticles was evaluated in HepG2 and Caco-2 cell lines, which mimic the *in vivo* the target of insulin-loaded SiNP upon oral administration.

2. Materials and methods

2.1. Materials

Tetraethyl orthosilicate (TEOS, 98%), NH_3 25%, PEG with M_w of 6000 and 20000 Da (PEG 6000; PEG 20000) were purchased from Merck (Darmstadt, Germany). Chitosan low molecular weight (235 g/mol, deacetylation degree of 78.5 %), ethanol 99.9 %, trehalose dehydrate and bovine serum albumin (BSA) were purchased from Sigma-Aldrich (Steinhein, Germany). Sodium alginate (198.11 g/mol) was purchased from VWR Portugal (Carnaxide, Portugal). Solution of 100 IU/mL of human insulin (Humulin® R) was purchased from Eli Lilly (Lisbon, Portugal). Dulbecco's Modified Eagle's Medium (DMEM), foetal bovine serum (FBS), penicillin/streptomycin, L-glutamine, 0.05% tripsin-EDTA and AlamarBlue (AB) were purchased from Gibco (Alfagene, Invitrogen, Portugal). HepG2 (Human hepatocellular carcinoma cell line; ATCC® Number: HB-8065 ™) were a gift from Professor Carlos Palmeira (CNC-UC, Coimbra, Portugal) and Caco-2 (Human colon adenocarcinoma cell line) was purchased from Cell Lines Service (CLS, Eppelheim, Germany). Ultra-purified water was obtained from MiliQ Plus system (Milipore, Germany).

2.2. Synthesis of nanoparticles

Silica nanoparticles were synthesized at room temperature via hydrolysis and condensation of TEOS under high shear homogenization (Ultra-Turrax, IKA, T25) using NH_3 as catalytic agent. The obtained nanoparticles were centrifuged and washed with a mixture of ethanol and ultra-purified water (1:1, v/v) by 2 cycles at 12,000 rpm for 5 min (Spectrafuge16M, Lambnet International, Inc.).

For coating silica nanoparticles, a solution of chitosan (CH) (0.3%, w/v) at pH 4.5, or sodium alginate (SA) (0.3% , w/v) at pH 4.5, or PEG 60002 or PEG 20000 (2%, w/v) at pH 6.8 was added to the nanoparticles, stirred for 30 min and centrifuged as described above.

For insulin association to SiNP, 1 mL of human insulin (100 IU/mL, pH 7.0) was added to 10 mg of uncoated SiNP under gentle stirring (300 rpm) for 30 min into ice bath.

For coated insulin-SNP, 1.0 mL of human insulin (100 IU/mL, pH 7.0) was dissolved in 2 mL of the hydrophilic polymer solutions, mixed for 30 min under magnetic stirring and then added to SiNP (10 mg) under gentle stirring (300 rpm) for more 30 min into ice bath. The nanoparticles were centrifuged at 5000 rpm for 5 min and the pellet was freeze-dried during 24 h in the presence of trehalose (10 %, w/v).

2.3. Differential Scanning Calorimetry (DSC) analysis

Thermograms were obtained using a TA Instrument (New Castle, USA). Accurately, 5 mg of lyophilized nanoparticles were weighted in 40 µL aluminium pans. DSC scans have been recorded from 25 to 350ºC at a heating constant rate of 10ºC/min under purging of nitrogen at 20 mL/min using an empty pan as reference. Data were obtained from the peaks areas using the TA software (TA Instrument).

2.4. Fourier Transform Infrared (FTIR) analysis

FTIR-spectra were performed using a Shimadzu® Europe - Prestige-21 spectrometer. Uncoated and coated nanoparticles containing insulin were gently mixed with a suitable amount of micronized KBr powder and compressed into discs at a force of 10 kN using a manual tablet presser. For each spectrum, a 128-scan interferogram was collected with a 4 cm^{-1} resolution in the mid-IR region at 25 °C.

2.5. X-Ray studies

X-Ray diffraction patterns of bulk materials and nanoparticles were performed using Siemens D5000 diffractometer system (Siemens, Germany) with a copper anode(Cu-Kα radiation, $\lambda = 0.1542$ nm) at angles $2\theta = 4\text{-}70^{\circ}$.

2.6. Cell cultures and maintenance

HepG2,a human hepatocellular carcinoma cell line, obtained from ATCC, was kindly provided by Prof. Carlos Palmeira (CNC, UC, Portugal) and Caco-2, a human colorectal adenocarcinoma cell line, obtained from Cell Line Services, AG (Germany)were used as cell models to perform the cytotoxicity assay of the different nanoparticles. HepG2

and Caco-2 cells were maintained in DMEM (Dulbecco's Modified Eagle Medium) supplemented with 10 % (v/v) foetal bovine serum (FBS), antibiotics (100 U/mL of penicillin and 100 µg/mL of streptomycin) and 1 mM L-glutamine in an atmosphere of 5% CO_2 /95 % air, at 37 °C with controlled humidity.

2.7. *In vitro* cytotoxicity assay

The cytotoxicity of nanoparticles was evaluated by comparing the proliferation rate and viability of non-exposed HepG2 or Caco-2 cells(control) with exposed HepG2 or Caco-2 cells, to appropriate concentrations during defined periods of time (see below), using the AB reduction method.

For the cytotoxicity assay cells were detached from the culture flaks with trypsin, counted and seeded into 96-well microplates at a density of 5×10^4 cells/mL (100 µL/well). Lyophilized nanoparticles were diluted in FBS-free culture media to various concentrations, ranging from 50 to 500 µg/mL (0, 50, 200, 500 µg/mL). Then, 24 h after seeding, the culture media was removed and replaced by media containing the nanoparticles (at defined concentrations). For each concentration of nanoparticles, microplates were placed in the incubator, and cells were exposed for 48 h. After the exposure time, the media containing the nanoparticles (and the control) was removed and replaced by FBS-free medium supplemented with 10 % (v/v) of AB. The absorbance readings occurred about 4 h after AB addition, at 570 and 620 nm using a Multiskan EX microplate reader (MTX Labsystems, USA). The percentage of AB reduction was calculated according to the following equation:

$$\%\ AB\ reduction = \frac{(\varepsilon_{ox}\lambda_2)(A\lambda_2) - (\varepsilon_{ox}\lambda_2)(A\lambda_2)}{(\varepsilon_{red}\lambda_1)(\acute{A}\lambda_2) - (\varepsilon_{red}\lambda_2)(\acute{A}\lambda_1)}\ x\ 100$$

where, $\varepsilon_{ox}\lambda_1$ is the molar extinction coefficient of oxidized AB at 570 nm, $\varepsilon_{ox}\lambda_2$ is the molar extinction coefficient of oxidized AB at 620 nm, $\varepsilon_{red}\lambda_1$ is the molar extinction coefficient of reduced AB at 570 nm, $\varepsilon_{red}\lambda_2$ is the molar extinction coefficient of reduced AB at 620 nm, $A\lambda_1$ and $A\lambda_2$ are the absorbance of test wells at 570 and 620 nm, respectively, and $\acute{A}\lambda_1$ and $\acute{A}\lambda_2$are the absorbance of the negative control wells (media plus AB but no cells) at 570 and 620 nm, respectively.

2.8. Statistical analysis

Results are expressed in terms of cell viability as percentage of control (untreated cells), and are a mean of three independent experiments (n=3) ± S.D (in each experiment, each condition was tested in 8 replicate wells (octuplicates)). Statistically evaluation of data was performed using a one-way analysis of variance (ANOVA) test. Bonferroni's Multiple Comparison test was carried out to compare the significance between the different groups. A p-value < 0.05 was considered statistically significant.

3. Results and discussions

3.1. DSC analysis

In this study, DSC was used to evaluate the influence of the selected coatings in SiNP. Table 1 presents a summary of the peak temperature and enthalpies associated with each peak for the various bulk materials and for the nanoparticles produced by sol-gel technology.

Typical DSC thermograms of coated SiNP with sodium alginate, SiNP-SA, chitosan, SiNP-CH, PEG 6000, SiNP-PEG 6000, and PEG 20000, SiNP-PEG 20000, are shown in Figure 1A (as denoted). Thermogram of sodium alginate depicted an endothermic peak at 97 ºC followed by an exothermic transition at 239.74 ºC (Table 1). The exothermic peaks attributed to a polymer were attributed to the degradation phenomena due to depolymerization or oxidation reactions [22, 23].

[Please, insert Table 1 near here]

Upon coating of SiNP with SA (SiNP-SA), the endothermic peak was shifted to 139.91 °C associated to an enthalpy of 65.41 J/g (Figure 1A, Table 1). Also, the addition of SA onto SiNP surface shifted the exothermic peak to higher temperatures, in comparison to SA alone. The shift of melting point and the exothermic peak in SiNP-SA may ascribe to the interaction between silica and sodium alginate resulting in higher thermal stability of the system. The second endothermic peak, at 253.51 °C, was attributed to the removal of the absorbed water in the sample under heating.

[Please, insert Figure 1 near here]

From the DSC results, Ins-SiNP-SA (Figure 1B and Table 1) showed the endothermic peak at different temperature values comparing to that obtained with unloaded nanoparticles (Figure 1A). The endothermic peak started at lower temperature, confirming that the presence of insulin changes the thermal behavior of nanoparticles due to the interaction between the protein and the polymer.

As indicated on Table 1, chitosan exhibits a sharp endothermic event, ascribing to the melting peak around 88.94 ºC and an exothermic event at 304.03 ºC. The coating of SiNP with chitosan (Figure 1A) changed the thermal behavior of the polymer with respect to the bulk material, shifting the endothermic transition to higher temperatures (93.05 °C), indicating the formation of strong hydrogen bonding between silica and chitosan [24]. To note, the exothermic peak of chitosan disappeared. Upon insulin association to SiNP-CH (Figure 1B), the endothermic peak is still present, almost unmodified. It can be concluded that the coating of SiNP with chitosan resulted in higher stability of the system, requiring more energy to break the interactions between silica and the polymer, as well as during the thermal decomposition of the nanoparticles. Again, the second endothermic peak at 204.98 ºC observed after coating with chitosan was due to the removal of adsorbed water. No signal of insulin peak was detectable after its incorporation in SiNP-CH, suggesting that insulin is completely dissolved in the polymer chains leading to an interaction between insulin and the polyelectrolyte (Figure 1; Table 1).

Concerning the effect of PEGylation on SiNP, the thermal behavior of nanoparticles using PEG 6000 was similar to that using PEG 20000 (Figure 1A). Pure PEG 6000 and PEG 20000 melt at 63.04 and 54.43 ºC, respectively (Table 1). The coating of SiNP with PEG 6000 and PEG 20000 shifted the endothermic peaks of the polymers to higher temperatures about 83.41 ºC and 94.84 ºC, respectively (Figure 1A). This result was attributed to the fact that PEG chains, in PEG-SiNP, are less flexible than those in pure PEG due to the interaction between silica and PEG segments (Figure 1A, Table 1). SiNP could act as nucleating agent, promoting the orientation of PEG chains and consequently leading to the high formation of crystal. In the presence of insulin, the endothermic peaks were registered at 92.10 °C for Ins-SiNP-PEG 6000 (Figure 1B) and at 102.17 °C for Ins-SiNP-PEG 20000 (Figure 1B). However, the peak recorded around

50 ºC, observed in both formulations, can be related to the transition midpoint (T_m) of insulin. T_m of insulin in the absence of nanoparticles was found to be 77.64 ºC (data not shown). Therefore, it is clear that PEG decreased the thermal stability of insulin. These results are in agreement with other studies that indicate that PEGs interact with the protein molecules by hydrophobic interactions being responsible for the destabilization of the protein structure [25].

3.2. X-ray studies

X-ray diffraction spectra indicate that sodium alginate, chitosan, PEG 6000, and PEG 20000 are present as a crystalline material (data not shown). However, the intensity of the peaks in SiNP-coated with the polymers is decreased, reflecting less ordered structure of the nanoparticles (Figures 2A). The association of insulin to nanoparticles also supports high crystallinity of the nanoparticles in comparison to unloaded nanoparticles (Figures 2B). The solubilization of insulin into the polymer solutions may have a tendency to crystallize the formulations during storage, thus leading to a change in the physical properties of the nanoparticles.

[Please, insert Figure 2 near here]

3.3. FTIR analysis

Figure 3 shows the FTIR spectra relative to the Ins-SiNP-CH (a), Ins-SiNP-SA (b), Ins-SiNP-PEG 6000 (c), Ins-SiNP-PEG 20000 (d) and Ins-SiNP (e).

The FTIR spectra of Ins-SiNP (Figure 3 (e)) showed a peak of free O–H stretching vibration around 3500 cm^{-1} (H-bonded H_2O, hydroxyl terminals, H-bonded OH vibrations of alcohol and H-bonded Si–OH in chain), a peak of Si–O stretching vibration around 1040 cm^{-1}, a peak Si-OH at 980 cm^{-1}, and a peak of Si–O–Si bending around 600 cm^{-1} vibration [26, 27].

The spectra of Ins-SiNP-CH (Figure 3 (a)) showed the presence of peaks around 1600, 1500 and 1400 cm^{-1}, related to amide bond, to vibration of protonated amine group and $–CH_2$ bending, respectively. The absorption bands at 1000 cm^{-1} (skeletal vibrations involving the C–O stretching) are characteristics of its saccharide structure [28]. A

characteristic band at 3440 cm^{-1} was assigned to O–H stretching, indicating intermolecular hydrogen bonding which is overlapped in the same region to the stretching vibration of N–H.

The bands around 1600 and 1400 cm^{-1} present in the FTIR spectrum of Ins-SiNP-SA Figure 3 (b) are assigned to symmetric and asymmetric stretching vibrations of carboxylate salt groups. In addition, the bands around 1300 cm^{-1} (C–O stretching), 1100 cm^{-1} (C–C stretching) and 1000 cm^{-1} (C–O stretching) are attributed to its saccharide structure [29].

The representative FTIR spectra of Ins-SiNP-PEG 20000 (Figure 3 (c)) and Ins-SiNP-PEG 6000 (Figure 3 (d)) were quite similar. The region between 3300 and 3600 cm^{-1} corresponds to O–H stretching, the band ranging from 2800 to 2900 cm^{-1} corresponds to C–H stretching and the band between 1000 and 1200 cm^{-1} is assigned to C–O stretching. The addition of PEG increased the relative intensity of the OH band indicating the increase of degree of hydration of the samples [30].

[Please, insert Figure 3 near here]

Comparing the spectra, changes observed in the absorption band of O–H can be assumed as a possible interaction that would occur between OH groups of SiNP and OH groups of PEG, as well as between OH groups and carboxyl of alginate or amino groups of chitosan. These results suggest an effective interaction between silica and the polymers. Finally, a band indicative of amide I at 1645 cm^{-1} (C=O stretching) was observed in all samples, which is characterized by the presence of α-helical content [31].

3.4. *In vitro* cytotoxicity assay

In this study, the toxicity of the different nanoparticles was evaluated by the resazurin (Alamar Blue, AB) reduction assay using HepG2 and Caco-2 cell lines and results of cell viability are compared with those of non-exposed cells (control) in terms of % of control. Most authors consider that viability above 70% of the control is an indication of "no toxicity" or of a safe material, and only viability below 70% is considered toxic, as reviewed recently [32].

Caco-2 and HepG2 were exposed for 48 h to SiNP, to coated-SiNP and to insulin loaded coated-SiNP, and the obtained results are shown in the Figures 4, 5 and 6.

For the uncoated SiNP, cell viability ranged from 97.67 ± 0.19 % (for 50 μg/mL) to 108.97 ± 2.17 % (for 200 μg/mL) for Caco-2 cells (Figure 4A), and from 92.63 ± 1.04 % (for 50 μg/mL) to 101.45 ± 3.41 % (for 200 μg/mL) for HepG2 cells (Figure 4B). No statistical significant changes, compared with the control group, were observed in both cell lines and at all tested concentrations, after 48 h exposure to uncoated SiNP ($p > 0.05$). These results can be attributed to the surface charge of nanoparticles. In this case, SiNP have negative charge at pH 7. Several studies have reported that negatively charged nanoparticles exert very little or no toxicity on biological membranes, in comparison to positively charged particles [33]. In Figure 4, a slight decrease in cell viability is observed when cells are exposed to insulin-loaded nanoparticles, compared to control. The decrease is more evident in Caco-2 cells (Figure 4A) than in HepG2 cells (Figure 4B), but the differences are minimal (no more than a 10% of decrease, from control).

[Please, insert Figure 4 near here]

It is important to consider that the coating of the nanoparticles with chitosan (CH), sodium alginate (SA) or PEG may change the pattern of toxicity comparing with the free polymers. For SiNP coated with chitosan, the cell viability ranged from 76.68 ± 1.17 % (for 500 μg/mL) to 96.84 ± 0.97 % (for 50 μg/mL) for Caco-2 cell (Figure 5A) and from 85.99 ± 8.99 % (for 200 μg/mL) to 99.44 ± 2.91 % (for 50 μg/mL) for HepG2 cells (Figure 5B). As shown in Figure 5A, compared with the control group, all concentrations reduced significantly the cell viability ($p < 0.05$), although reduction in not higher than 25 %. Figure 5A also shows that cell viability is reduced with the increase in the nanoparticles concentration, leading to cytotoxicity being concentration dependent, and that loading SiNP-CH with insulin improves cell viability.

As observed in Figure 5B, HepG2 cell viability was less affected by nanoparticles exposure than Caco-2 cells. At 50 μg/mL SiNP-CH, changes in cell viability were not statistically significant, after 48 h exposure. Comparing with uncoated SiNP (Figure 4), it is observed that SiNP coated with chitosan (SiNP-CH) induced slightly higher toxicity in both cell lines (Figure 5A and B). *In vitro* evaluation of chitosan and chitosan nanoparticles has been performed in a wide range of cell lines demonstrating low

cytotoxicity [34, 35]. However, it is known that cationic compounds can cause cell damage. The presence of the positive charges on the SiNP-CH surface may consequently affects the interaction with cells leading to a decrease of cell viability. Many studies suggest that cationic materials imply higher toxicity due to the interactions with the plasmatic membrane and/or with negatively charged cell components and proteins [36-38]. Also, some works have showed that chitosan coated nanoparticles can induce cell apoptosis in some extend [39].

As observed in Figure 5A and 5B, insulin-loaded nanoparticles decreased the cytotoxicity of SiNP-CH, after 48 h of exposure, being more evident in Caco-2 cells at high concentrations. This phenomenon can be related to the possible decrease of the interaction between the positively charged amino groups of chitosan with the anionic components of the glycoproteins on the cell membrane surface, improving cell viability. Regarding to SiNP-SA, Caco-2 cells (Figure 5C) were also more susceptible than HepG2 cells (Figure 5D) to the exposure to SiNP-coated with sodium alginate. All concentrations of SiNP-SA significantly reduced the viability of Caco-2 cells, compared to control (Figure 5C), however, some reductions are minimal (no more than a 20% of decrease, from control). However, only the concentration of 500 μg/mL of SiNP-SA reduced significantly HepG2 viability (Figure 5D). Similar results were obtained by Douglas and co-workers [40], demonstrating that high concentrations of alginate-chitosan nanoparticles resulted in a significant decrease of 293 T cells viability after 24 h of incubation in comparison to chitosan polymer.

[Please, insert Figure 5 near here]

After insulin incorporation into SiNP-SA, all tested concentrations showed low cytotoxicity in Caco-2 (Figure 5C) and HepG2 cells (Figure 5D). As reported previously, insulin loading seems to improve cell viability. These results are in evident agreement with other studies demonstrating high biocompatibility of alginate as a coating or even as a carrier [41].

In general, we can observe a low degree of toxicity for all particles at the concentration range tested. However, for the unloaded nanoparticles, a reduction in the cell viability is observed which is concentration dependent, and it is more evident for Caco-2 cells, as observed for SiNP-CH (Figure 5A) and for SiNP-SA (Figure 5C).

Concerning the coating with PEG (Figure 6), two different PEG polymers were studied differing in chain extent and thus in MW, the PEG 6000 and PEG 20000 were used. Cell viability of Caco-2 (Figure 6A) and HepG2 cells (Figure 6B) after 48 h of exposure to SiNP-PEG 6000 and SiNP-PEG 20000 is shown. Concerning the effect of nanoparticles concentration on cytotoxicity, we could note that higher concentrations of SiNP-PEG 6000 (200 and 500 µg/mL) induced higher cytotoxicity in both cell lines (Figure 6A and 6B), to note that 500 µg/mL of SiNP-PEG 6000 reduced Caco-2 cell viability by more than 50% (Figure 6A). However, according to what has been already reported insulin-loading improves cell viability, and for all concentrations of Ins-SiNP-PEG 6000 viability is around 90%.

On the other hand, SiNP-PEG 20000 did not significantly affect the HepG2 or the Caco-2 cell viability (Figure 6B and 6A). In general, conjugation of PEG to nanoparticles is recognized as being nontoxic by all routes of administration. However, comparing to uncoated SiNP, the concentrations of 200 and 500 µg/mL of SiNP-PEG 6000, in both cell lines, reduced significantly cell viability. Cho and co-workers [42] showed that gold nanoparticles coated with PEG 5000 can induce acute inflammation and apoptosis in the mouse liver. Higher cell viability, especially at concentration of 200 and 500 µg/mL was observed for SiNP-PEG 20000 compared to that of SiNP-PEG 6000. This result can be attributed to the long chain structure of PEG 20000 leading to a higher steric effect. The flexibility of a long PEG chain like PEG 20000 was supposed to make it to cover greater surface area. Similar observations were obtained by Mao and co-workers [43] that verified lower cytotoxicity effect of trimethyl chitosan (TMC) grafted by PEG 5 kDa in comparison to TMC grafted by PEG 550 Da. However, some studies showed that low PEG chain length used for poly(ethylene imine) (PEI) coating induced low cytotoxic and oxidative stress response in lung cell line [44]. No cytotoxicity effect on cell proliferation and viability was observed after the incorporation of insulin into SiNP-PEG 6000 and SiNP-PEG 20000 for both cell lines (Figure 6).

4. Conclusions

DSC, X-ray and FTIR were used to evaluate the influence of different coatings in insulin-loaded SiNP. In the DSC studies, the endothermic and exothermic peaks of pure polymers were shifted to high temperature in all coated SiNP resulting in more stable systems. The X-ray diffraction showed that coated SiNP displayed less ordered

structure compared with pure polymers. On the other hand, the association of insulin to nanoparticles resulted in more crystalline structures. FTIR analysis also demonstrated the interaction between mucoadhesive polymers and nanoparticles. Additionally, the toxicity assay showed that different surface modification of SiNP did not affect, or affect in a low degree, the cell viability, demonstrating very low toxicity in Caco-2 and HepG2 cell lines, indicating that the developed nanoparticles are promising biocompatible for oral drug delivery systems.

Acknowledgments

The work was partially supported by Fundação para a Ciência e Tecnologia (FCT, Portugal), namely, the PhD scholarships SFRH/BD/60640/2009 for T. Andreani and SFRH/BD/80335/2011 for J.F. Fangueiro. FCTand FEDER/COMPETE funds are also acknowledged under the reference PTDC/SAU-FAR/113100/2009 and PEst-C/AGR/UI4033/2014. The authors acknowledge the support by Fundação de Amparo à Pesquisa do Estado de São Paulo (FAPESP) for the PhD scholarship for C.P. Kiill under the reference 2012/10174-3.

References

[1] F.-Y. Su, K.-J. Lin, K. Sonaje, S.-P. Wey, T.-C. Yen, Y.-C. Ho, N. Panda, E.-Y. Chuang, B. Maiti, H.-W. Sung, Protease inhibition and absorption enhancement by functional nanoparticles for effective oral insulin delivery, Biomaterials, 33 (2012) 2801-2811.

[2] N. Shrestha, M.-A. Shahbazi, F. Araújo, H. Zhang, E.M. Mäkilä, J. Kauppila, B. Sarmento, J.J. Salonen, J.T. Hirvonen, H.A. Santos, Chitosan-modified porous silicon microparticles for enhanced permeability of insulin across intestinal cell monolayers, Biomaterials, 35 (2014) 7172-7179.

[3] E.-S. Khafagy, N. Kamei, E.J.B. Nielsen, R. Nishio, M. Takeda-Morishita, One-month subchronic toxicity study of cell-penetrating peptides for insulin nasal delivery in rats, Eur J Pharm Biopharm, 85(2013) 736-743.

[4] S. Al-Qadi, A. Grenha, D. Carrión-Recio, B. Seijo, C. Remuñán-López, Microencapsulated chitosan nanoparticles for pulmonary protein delivery: In vivo evaluation of insulin-loaded formulations, J Control Release, 157 (2012) 383-390.

[5] K.P. Amancha, S. Balkundi, Y. Lvov, A. Hussain, Pulmonary sustained release of insulin from microparticles composed of polyelectrolyte layer-by-layer assembly, Int J Pharm, 466 (2014) 96-108.

[6] C. Giovino, I. Ayensu, J. Tetteh, J.S. Boateng, Development and characterisation of chitosan films impregnated with insulin loaded PEG-b-PLA nanoparticles (NPs): A potential approach for buccal delivery of macromolecules, Int J Pharm, 428 (2012) 143-151.

[7] J.O. Morales, S. Huang, R.O. Williams, J.T. McConville, Films loaded with Insulin-coated nanoparticles (ICNP) as potential platforms for peptide buccal delivery, Colloids Surf B Biointerfaces, 122 (2014) 38–45.

[8] S. Liu, M.-n. Jin, Y.-s. Quan, F. Kamiyama, H. Katsumi, T. Sakane, A. Yamamoto, The development and characteristics of novel microneedle arrays fabricated from hyaluronic acid, and their application in the transdermal delivery of insulin, J Control Release, 161 (2012) 933-941.

[9] D.R. Owens, B. Zinman, G. Bolli, Alternative routes of insulin delivery, Diabet Med, 20 (2003) 886-898.

[10] J. Hamman, G. Enslin, A. Kotzé, Oral delivery of peptide drugs, BioDrugs, 19 (2005) 165-177.

[11] Z. Deng, Z. Zhen, X. Hu, S. Wu, Z. Xu, P.K. Chu, Hollow chitosan-silica nanospheres as pH-sensitive targeted delivery carriers in breast cancer therapy, Biomaterials, 32 (2011) 4976-4986.

[12] D. Liu, X. He, K. Wang, C. He, H. Shi, L. Jian, Biocompatible silica nanoparticles-insulin conjugates for mesenchymal stem cell adipogenic differentiation, Bioconjug Chem, 21 (2010) 1673-1684.

[13] R.N. Jain, X. Huang, S. Das, R. Silva, V. Ivanova, T. Minko, T. Asefa, Functionalized mesoporous silica nanoparticles for glucose- and pH-stimulated release of insulin, Z Anorg Allg Chem, 640 (2014) 616-623.

[14] T. Andreani, A.L.R. Souza, C.P. Kiill, E.N. Lorenzón, J.F. Fangueiro, A.C. Calpena, M.V. Chaud, M.L. Garcia, M.P.D. Gremião, A.M. Silva, E.B. Souto, Preparation and characterization of PEG-coatedsilicananoparticlesfor oral insulindelivery, Int J Pharm, 473 (2014) 627-635.

[15] S.L. Westcott, S.J. Oldenburg, T.R. Lee, N.J. Halas, Formation and adsorption of clusters of gold nanoparticles onto functionalized silica nanoparticle surfaces, Langmuir, 14 (1998) 5396-5401.

[16] L. Yin, J. Ding, C. He, L. Cui, C. Tang, C. Yin, Drug permeability and mucoadhesion properties of thiolated trimethyl chitosan nanoparticles in oral insulin delivery, Biomaterials, 30 (2009) 5691-5700.

[17] Schipper NG, Olsson S, Hoogstraate JA, deBoer AG, Varum KM, A. P., Chitosans as absorption enhancers for poorly absorbable drugs 2: mechanism of absorption enhancement, Pharm Res, 14 (1997) 923-929.

[18] K. Park, J.R. Robinson, Bioadhesive polymers as plataforms for oral-controlled drug delivery: Method to study bioadhesion, Int J Pharm, 19 (1984) 107-127.

[19] M. Tobío, A. Sánchez, A. Vila, I. Soriano, C. Evora, J.L. Vila-Jato, M.J. Alonso, The role of PEG on the stability in digestive fluids and in vivo fate of PEG-PLA nanoparticles following oral administration, Colloids Surf B, 18 (2000) 315-323.

[20] N.A. Peppas, Molecular calculations of poly(ethyleneglycol) transport across a swollen poly(acrylicacid)/mucin interface, J Biomater SciPolymer Edn, 9 (1998) 535-542.

[21] V.V. Ginzburg, S. Balijepalli, Modeling the thermodynamics of the interaction of nanoparticles with cell membranes, Nano Lett, 7 (2007) 3716-3722.

[22] T. Mimmo, C. Marzadori, D. Montecchio, C. Gessa, Characterisation of Ca- and Al-pectate gels by thermal analysis and FTIR spectroscopy, Carbohydr Res, 340 (2005) 2510-2519.

[23] M.J. Zohuriaan, F. Shokrolahi, Thermal studies on natural and modified gums, Polymer Testing, 23 (2004) 575-579.

[24] S.M. Lai, A.J.M. Yang, W.C. Chen, J.F. Hsiao, The Properties and Preparation of Chitosan/Silica Hybrids Using Sol-Gel Process, Polym Plast Technol Eng, 45 (2006) 997-1003.

[25] T. Arakawa, S.N. Timasheff, Mechanism of poly(ethyeleneglycol) interaction of proteins, Biochemistry 24 (1985) 6756-6762.

[26] K. Kusakabe, K. Ichiki, J.-I. Hayashi, H. Maeda, S. Morooka, Preparation and characterization of silica-polyimide composite membranes coated on porous tubes for CO2 separation, J Membr Sci, 115 (1996) 65-75.

[27] A. Kioul, L. Mascia, Compatibility of polyimide-silicate ceramers induced by alkoxysilane coupling agents, J Non-Cryst Solids, 175 (1994) 169–186.

[28] Y.J. Yin, K.D. Yao, G.X. Cheng, J.B. Ma, Properties of polyelectrolyte complex films of chitosan and gelatin, Polym Int, 48 (1999) 429-432.

[29] C. Sartori, D.S. Finch, B. Ralph, K. Gilding, Determination of the cation content of alginate thin films by FTIR spectroscopy, Polymer, 38 (1997) 43-51.

[30] M. Prokopowicz, J. Łukasiak, Synthesis and in vitro characterization of freeze-dried doxorubicin-loaded silica/PEG composite, J Non-Cryst Solids, 356 (2010) 1711-1720.

[31] X.G. Zhang, D.Y. Teng, Z.M. Wu, X. Wang, Z. Wang, D.M. Yu, C.X. Li, PEG-grafeted chitosan nanoparticles as a injectable carrier for sustained protein release, J Mater Sci Mater Med, 19 (2008) 3525-3533.

[32] S. Doktorovova, E.B. Souto, A.M. Silva, Nanotoxicology applied to solid lipid nanoparticles and nanostructured lipid carriers – A systematic review of in vitro data, Eur J Pharm Biopharm, 87 (2014) 1-18.

565 [33] S. Bhattacharjee, L. de Haan, N. Evers, X. Jiang, A. Marcelis, H. Zuilhof, I.
566 Rietjens, G. Alink, Role of surface charge and oxidative stress in cytotoxicity of
567 organic monolayer-coated silicon nanoparticles towards macrophage NR8383 cells,
568 Particle Fibre Toxicol, 7 (2010) 25.

569 [34] M. Huang, E. Khor, L.-Y. Lim, Uptake and Cytotoxicity of Chitosan Molecules
570 and Nanoparticles: Effects of Molecular Weight and Degree of Deacetylation, Pharm
571 Res, 21 (2004) 344-353.

572 [35] D. Jeevitha, K. Amarnath, Chitosan/PLA nanoparticles as a novel carrier for the
573 delivery of anthraquinone: Synthesis, characterization and in vitro cytotoxicity
574 evaluation, Colloids Surf B, 101 (2014) 126-134.

575 [36] S. Choksakulnimitr, S. Masuda, H. Tokuda, Y. Takakura, M. Hashida, In vitro
576 cytotoxicity of macromolecules in different cell culture systems, J Control Release,
577 34 (1995) 233-241.

578 [37] D. Fischer, Y. Li, B. Ahlemeyer, J. Krieglstein, T. Kissel, In vitro cytotoxicity
579 testing of polycations: influence of polymer structure on cell viability and hemolysis,
580 Biomaterials, 24 (2003) 1121-1131.

581 [38] J.F. Fangueiro, T. Andreani, M.A. Egea, M.L. Garcia, S.B. Souto, A.M. Silva, E.B.
582 Souto, Design of cationic lipid nanoparticles for ocular delivery: Development,
583 characterization and cytotoxicity, Int J Pharm, 461 (2014) 64-73.

584 [39] L. Zhu, J. Ma, N. Jia, Y. Zhao, H. Shen, Chitosan-coated magnetic nanoparticles as
585 carriers of 5-Fluorouracil: Preparation, characterization and cytotoxicity studies,
586 Colloids Surf B, 68 (2009) 1-6.

587 [40] K.L. Douglas, C.A. Piccirillo, M. Tabrizian, Effects of alginate inclusion on the
588 vector properties of chitosan-based nanoparticles, J Control Release, 115 (2006) 354-
589 361.

590 [41] O. Borges, A. Cordeiro-da-Silva, S.G. Romeijn, M. Amidi, A. de Sousa, G.
591 Borchard, H.E. Junginger, Uptake studies in rat Peyer's patches, cytotoxicity and
592 release studies of alginate coated chitosan nanoparticles for mucosal vaccination, J
593 Control Release, 114 (2006) 348-358.

594 [42] W.-S. Cho, M. Cho, J. Jeong, M. Choi, H.-Y. Cho, B.S. Han, S.H. Kim, H.O. Kim,
595 Y.T. Lim, B.H. Chung, J. Jeong, Acute toxicity and pharmacokinetics of 13 nm-sized
596 PEG-coated gold nanoparticles, Toxicol Appl Pharmacol, 236 (2009) 16-24.

597 [43] S. Mao, X. Shuai, F. Unger, M. Wittmar, X. Xie, T. Kissel, Synthesis,
598 characterization and cytotoxicity of poly(ethyleneglycol)-graft-trimethylchitosan
599 block copolymers, Biomaterials 26 (2005) 6343-6356.

600 [44] A. Beyerle, O. Merkel, T. Stoeger, T. Kissel, PEGylation affects cytotoxicity and
601 cell-compatibility of poly(ethyleneimine) for lung application: Structure–function
602 relationships, Toxicol Appl Pharmacol, 242 (2010) 146-154.

603

603

604 **Figure Caption**

605

606 **Figure 1.** DSC thermograms. (**A**) SiNP coated with sodium alginate (SA), chitosan
607 (CH), PEG 6000 or PEG 20000, as indicated. (**B**) SiNP coated with sodium alginate
608 (SA), chitosan (CH), PEG 6000 or PEG 20000 after insulin association, as indicated.

609

610 **Figure 2.** X-ray diffraction patterns of (**A**) SiNP coated with sodium alginate (SA),
611 chitosan (CH), PEG 6000 or PEG 20000; (**B**) of SiNP coated with sodium alginate
612 (SA), chitosan (CH), PEG 6000 or PEG 20000 after insulin association, as indicated.

613

614 **Figure 3.** FTIR spectra of (a) Ins-SiNP-CH, (b) Ins-SiNP-SA, (c) Ins-SiNP-PEG 20000,
615 (d) Ins-SiNP-PEG 6000 and (e) Ins-SiNP.

616

617 **Figure 4.** Viability of Caco-2 (A) and HepG2 (B) cells after 48 h exposure to 50, 100,
618 200 and 500 μg/mL of uncoated and unloaded SiNP, (white bars) and uncoated insulin-
619 loaded (grey bars). Cell viability is expressed as % of control, being the mean of 3
620 different experiments ± S.D.. For each cell line, three independent experiments (each
621 with 8 replicates) were carried out.

622

623 **Figure 5.** Effect of coating SiNP with chitosan (CH) or sodium alginate (SA) on cell
624 viability.Caco-2 cells (A) and HepG2 cells (B) were exposed to empty chitosan coated
625 SiNP (SiNP-CH; white bars) and to insulin loaded SiNP-CH (Ins-SiNP-CH; dark-grey
626 bars). In different experiments, Caco-2 cells (C) and HepG2 cells (D) were exposed to
627 SA-coated empty SiNP (SiNP-SA; light grey bars) or to insulin-loaded SiNP-SA(Ins-
628 SiNP-SA; black bars). All cells were exposed to the respective NP for 48 h at 50, 100,

200 and 500 μg/mL, as denoted. Cell viability is expressed as % of control, being the mean of 3 different experiments ± S.D. For each cell line, three independent experiments (each with 8 replicates) were carried out.

Figure 6. Effect of PEGylation of SiNP on the cell viability of Caco-2 (A) and HepG2 (B) cells using PEG 6000 and PEG 20000, as indicated. Cells were exposed for 48 h to 50, 100, 200 and 500 μg/mL with coated-SiNP and insulin-loaded coated-SiNP, as denoted. Cell viability is expressed as % of control being the mean of 3 different experiments ± S.D. For each cell line, three independent experiments (each with 8 replicates) were carried out.

Table Caption

Table 1.DSC parameters of the polymers and unloaded and loaded-nanoparticles produced by sol-gel technology.

646 **Table Caption**

647

648 **Table 1.** DSC parameters of the polymers and unloaded and loaded-nanoparticles
649 produced by sol-gel technology.

650

651 **Table 1.**

Samples	Temperature (ºC)			*ΔH* (J/g)
	Initial	Peak	Final	
PEG 6000	58.50	63.04	73.57	163.40
PEG 20000	51.97	54.43	62.95	101.70
Sodium alginate	43.99	97.00	153.31	238.00
	220.78	239.74	273.67	202.70
Chitosan	45.17	88.94	139.72	124.40
	286.32	304.03	338.78	117.00
SiNP-PEG 6000	32.05	83.41	133.08	89.24
	268.72	287.30	347.28	145.40
SiNP-PEG 20000	40.84	94.84	159.43	123.40
	263.37	287.89	347.07	209.60
SiNP-SA	77.65	139.91	199.85	65.41
	210.11	253.51	279.06	26.69
	282.50	311.55	345.00	120.10
SiNP-CH	40.09	93.05	155.48	94.81
	201.29	229.84	306.84	126.20
Ins-SiNP-PEG 6000	59.63	92.10	114.01	128.70
Ins-SiNP-PEG 20000	69.28	101.17	142.21	146.10
Ins-SiNP-SA	78.23	102.16	129.77	132.30
	287.90	292.99	297.72	53.43
Ins-SiNP-CH	53.41	91.29	150.92	234.80
	193.02	204.98	230.12	133.30

652

653

653 1) Hybrid nanoparticles were produced by Stöber method for insulin association
654 2) Silica nanoparticles were coated with chitosan, sodium alginate or PEG
655 3) Coating of silica nanoparticles resulted in more stable systems
656 4) PEGylated nanoparticles decreased the thermal stability of insulin
657 5) In general, all nanoparticles showed low toxicity in Caco-2 and HepG-2 cells
658

1) Production of coated-SiNP for insulin association

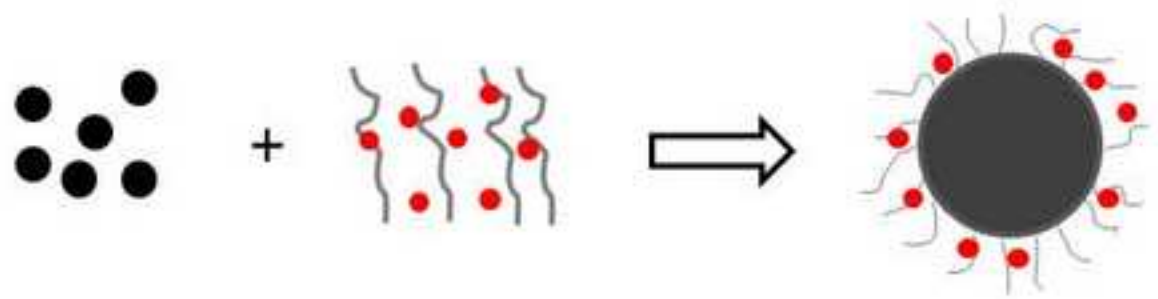

2) Characterization of nanoparticles

- Thermal analysis
- Crystallinity
- FTIR analysis

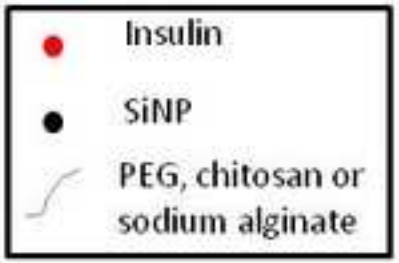

3) Biocompatibility of nanoparticles

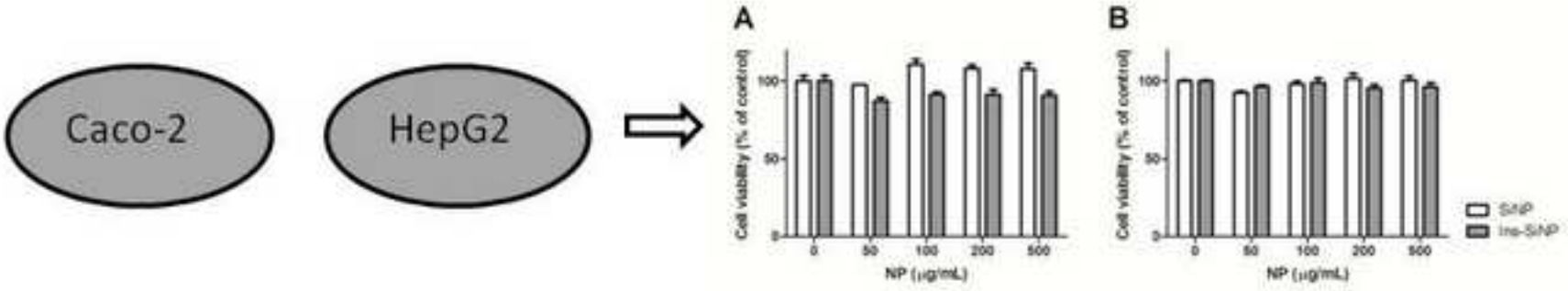

Figure 1.

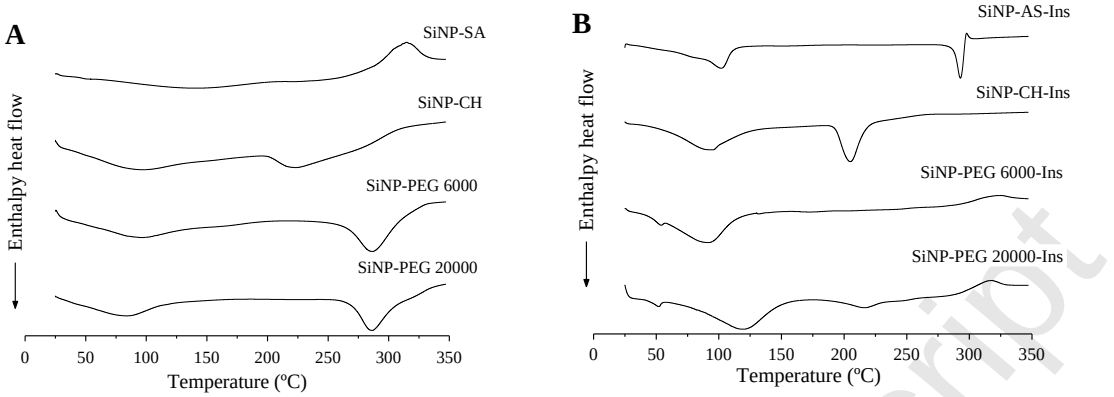

Figure 2.

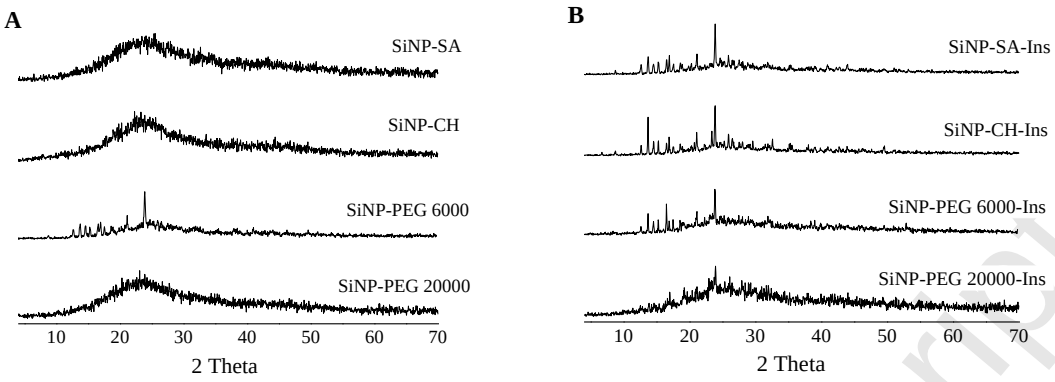

Figure 3.

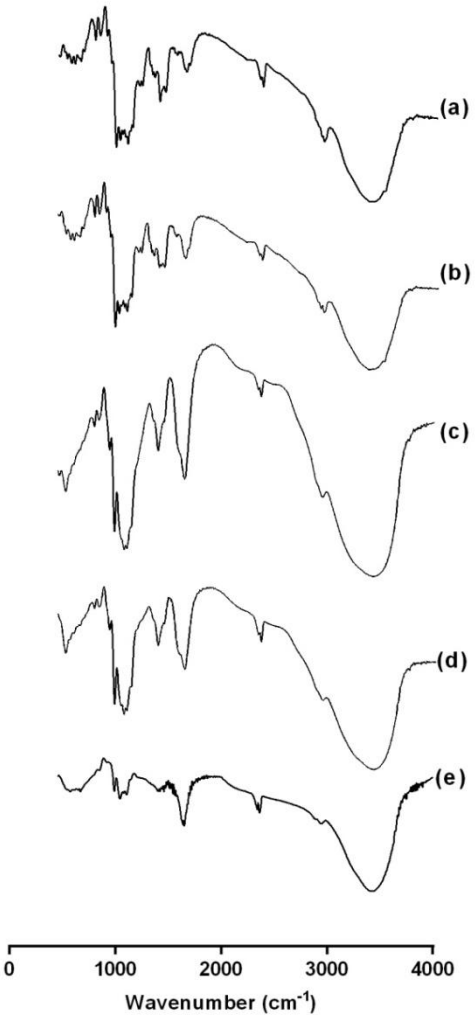

Figure(s)

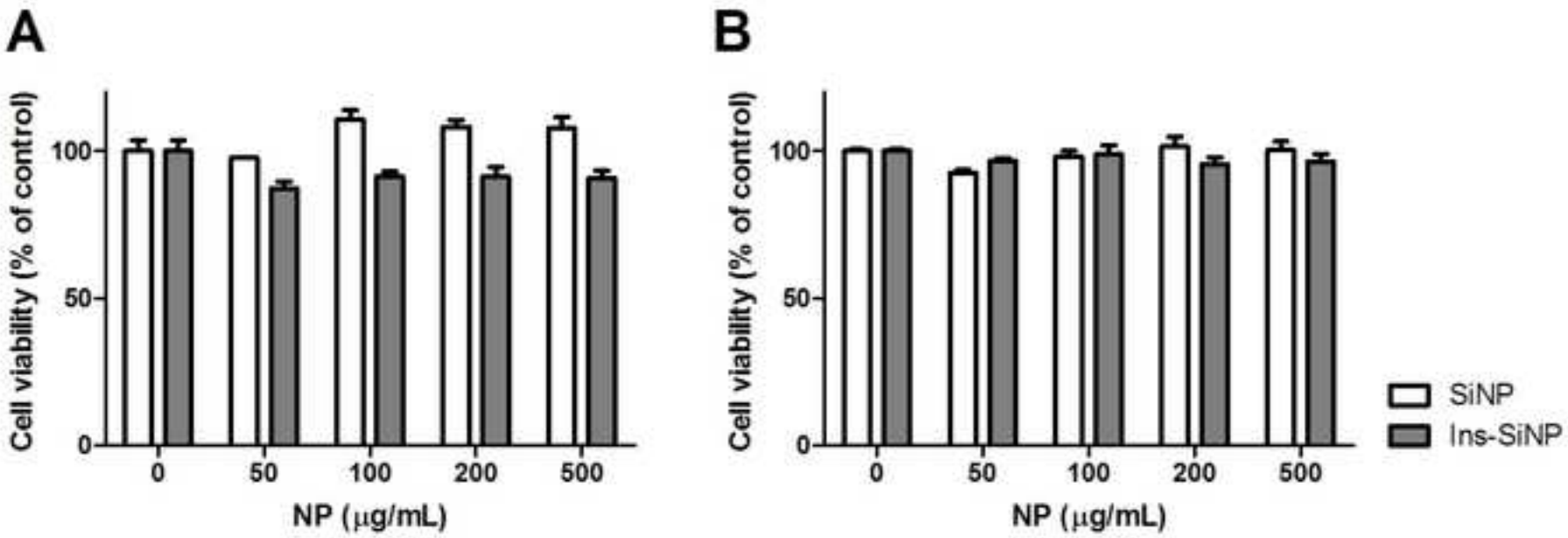
A
B
Cell viability (% of control)
100
50
0
0
50
100
200
500
NP (μg/mL)
SiNP
Ins-SiNP

Figure(s)

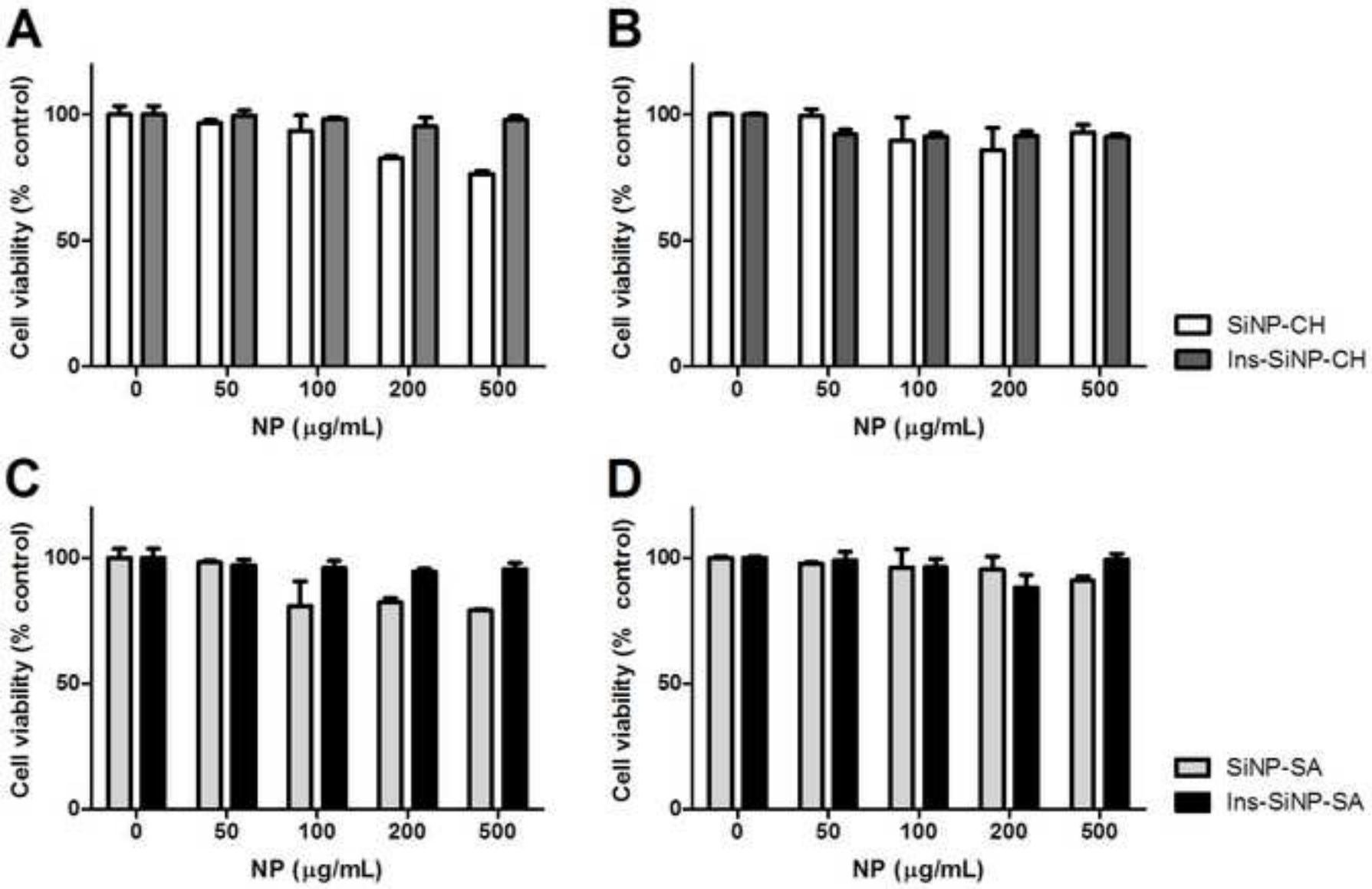
A
B
C
D
Cell viability (% control)
100
50
0
0
50
100
200
500
NP (μg/mL)
SiNP-CH
Ins-SiNP-CH
SiNP-SA
Ins-SiNP-SA

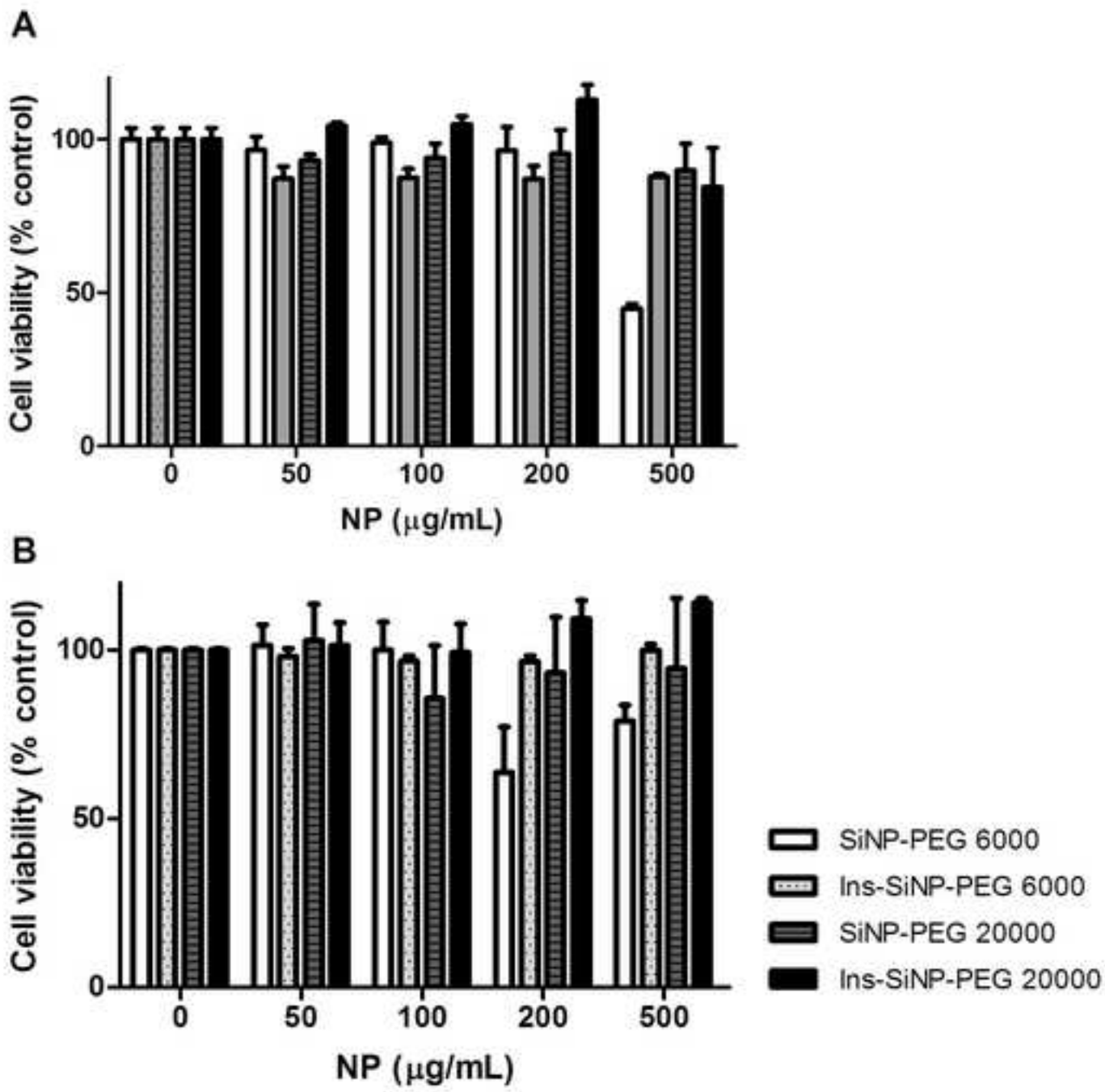
A
Cell viability (% control)
100
50
0
0
50
100
200
500
NP (μg/mL)
B
Cell viability (% control)
100
50
0
0
50
100
200
500
NP (μg/mL)
SiNP-PEG 6000
Ins-SiNP-PEG 6000
SiNP-PEG 20000
Ins-SiNP-PEG 20000